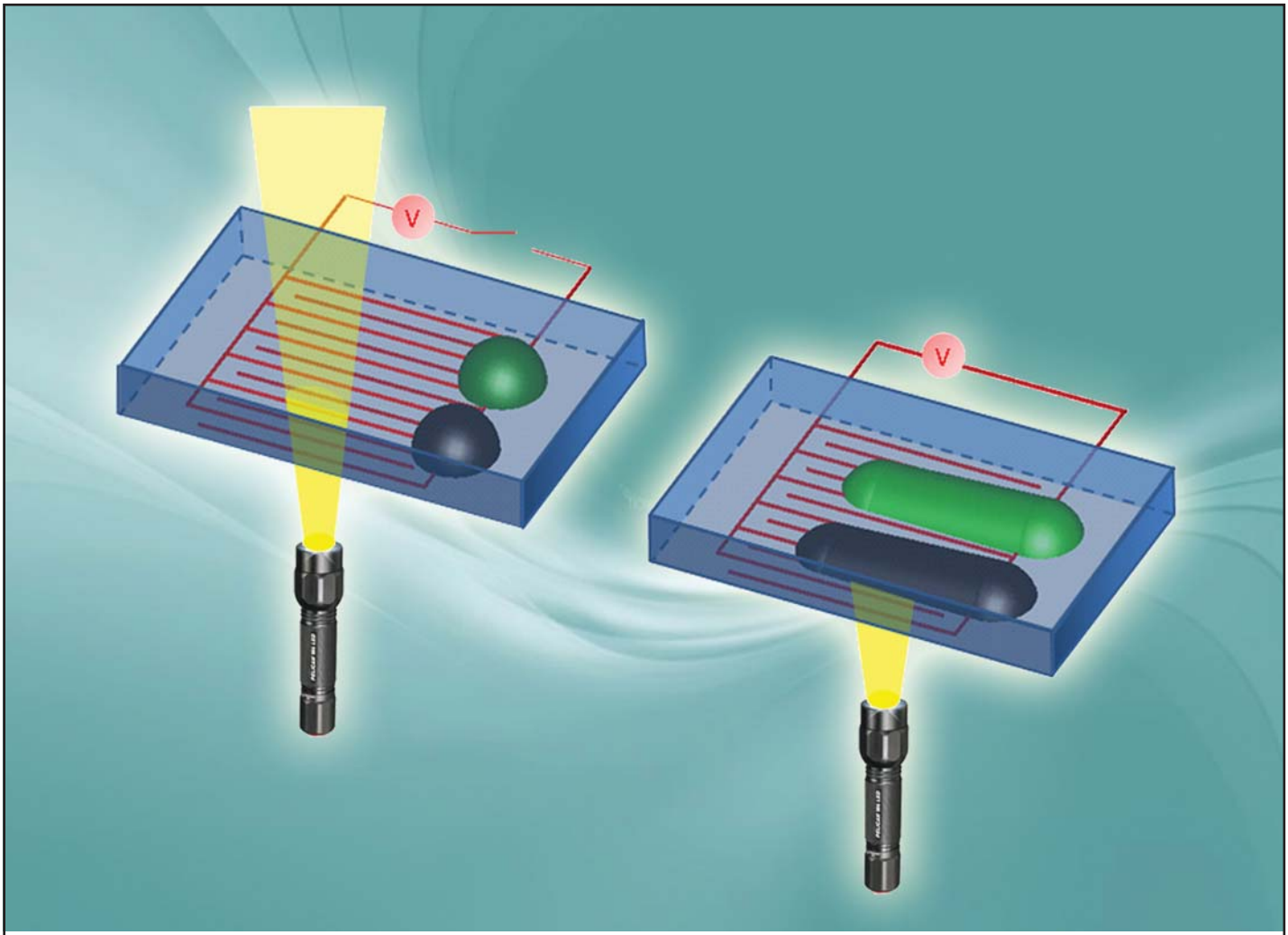

Featuring research from the groups of Professor Hongwen Ren at Chonbuk National University, Republic of Korea and Professor Shin-Tson Wu at the University of Central Florida, USA.

Title: Voltage-expandable liquid crystal surface

Fringing electric field can spread a ball-shaped liquid droplet to a film-like layer. Such a result may find numerous applications in high performance optical switches, displays, and other lab-on-a chip devices.

As featured in:

See Ye and Demirci *et al.*, *Lab Chip*, 2011, **11**, 3411.

RSC Publishing

www.rsc.org/loc

Registered Charity Number 207890

Lab on a Chip

Dynamic Article Links

Cite this: *Lab Chip*, 2011, **11**, 3426

www.rsc.org/loc

PAPER

Voltage-expandable liquid crystal surface†

Hongwen Ren,*[a] Su Xu[b] and Shin-Tson Wu[b]

Received 2nd May 2011, Accepted 27th July 2011
DOI: 10.1039/c1lc20367c

Based on dielectrophoretic effect, we report a novel approach which can extensively spread a liquid crystal (LC) interface. With interdigitated striped electrodes, the droplets can be stretched along the striped electrode direction; while with zigzag interdigitated electrodes, the droplets can be further stretched sidewise. In our demonstration, the occupied area of a 1.9-mm-aperture LC droplet doped with 1.2 wt% black dye could be expanded over ~3.5× at 78 V_{rms}. The spreading and recovering times were measured to be ~0.39 s and ~0.75 s, respectively. The slower response time confirms the extreme expanding of the LC surface. The contrast ratio is over ~120 : 1 in transmissive mode. Color light switch was also demonstrated by spreading colored-dye doped LC droplets. The mechanical stability of the device was also evaluated. Liquid devices based on this cell structure have the advantages of good stability, simple operation and low power consumption. This work opens a new gateway for voltage controllable, polarization-insensitive, and broadband liquid photonic devices which may find numerous applications in switchable windows, variable optical attenuators, and displays.

Introduction

Optical switches have been studied intensively in the past years. Twisted-nematic liquid crystal (TNLC) should be the most successive approach for various optical switches.[1] However, two polarizers are required for a TNLC device, so the light efficiency is below 50%. In comparison to TNLC, a liquid with its surface reconfigurable also exhibits the properties of optical control. Depending on the surface profile, the liquids have found widespread applications in adaptive focus,[2–7] variable optical attenuators,[8,9] beam steering,[10,11] adaptive iris,[12] and displays.[13,14] The common merits of those devices are that they do not need any polarizers.

To reshape the liquid surface, various mechanisms have been developed.[2–7,15,16] Electrowetting and dielectrophoresis (DEP) are attractive because of direct voltage actuation. In an electrowetting cell, one liquid forms a droplet on one substrate surface, and another liquid fills its outside space. The two liquids are immiscible and one of them is conductive. When a voltage is applied to the cell, the shape change of the droplet obeys Young–Lippmann's theory: increasing the voltage can decrease the contact angle of the droplet.[17] The decrease of contact angle will cause the shape of the droplet to be flat. However, in a real case, when the voltage is high enough, the contact angle has a tendency to be saturated. The Young–Lippman' equation does not predict the saturation of the contact angle and this phenomena is still not clear. Due to this reason, a hydrophobic surface is needed so that the liquid droplet exhibits the smallest surface to volume ratio. Even so, the surface profile of the liquid droplet could not be largely expanded, especially for a large-sized droplet.

Unlike electrowetting, both liquids in a DEP cell are insulated but with different dielectric constants. In our previous work, the voltage applied to the cell is in a longitudinal direction, and the gradient electric field is induced by the droplet itself because of the curved surface.[7,9] The cell usually needs a high operating voltage to deform the droplet shape even though its size is quite small. In a liquid device with zone-patterned electrodes, the operating voltage is independent of the cell gap.[6] However, the droplet deformation is limited. Because the border of the droplet will periodically meet the circulated valley of the electric field during shape deformation, a high voltage is required in order to enhance the gradient of electric field falling on the droplet border. Except for the adaptive lens and prism, DEP has been widely used to wave the dielectric liquid surface,[18] manipulate dielectric particles,[19] separate cells,[20] or move microsized droplets in microfluidic channels.[21–23] However, few are about expanding the shape of a large liquid droplet. It is a challenge to extremely expand the shape of a liquid droplet using conventional approaches and materials.

Here we report using a fringing field to stretch a dye-doped liquid crystal (LC) droplet. In the relaxing state, the droplet shrinks with the smallest surface to volume ratio. In the actuation state, the generated DEP force can expand the droplet surface and a film-like shape can be obtained. Droplets with

[a]*Department of Polymer Nano Science and Engineering, Chonbuk National University, Jeonju, South Korea. E-mail: hongwen@jbnu.ac.kr; Fax: +82-63-270-2341; Tel: +82-63-270-2354*
[b]*College of Optics and Photonics, University of Central Florida, Orlando, USA. E-mail: suxu@creol.ucf.edu; swu@mail.ucf.edu; Fax: +407-823-6880; Tel: +407-823-4763*

† Electronic supplementary information (ESI) available: Supplemental Movie 1 and 2. See DOI: 10.1039/c1lc20367c

various apertures were prepared and their dynamic responses were measured. Black dye-doped droplets exhibit a good contrast ratio (~120 : 1) and high aperture ratio (~75%). The response speed is also reasonable. Color light switch was also demonstrated by spreading colored-dye doped LC droplets. Devices based on our cell can be easily fabricated without the concern of controlling cell gap. By using fringing field, the voltage is independent of the cell gap. Therefore, the size of the droplet is scalable. This work opens a new gateway for voltage controllable, polarization-insensitive, and broadband liquid photonic devices, such as optical switches, displays, and other lab-on-a-chip applications.

Device structure and basic theory

Fig. 1 shows our proposed device structure. The side-view (Fig. 1a) shows the droplet liquid-1 and the outside liquid-2 sandwiched between two glass substrates. The surface of the bottom glass plate is coated with indium tin oxide (ITO) electrode. The ITO electrode is etched with interdigitated strips. On the top of the electrodes is a thin hole-patterned dielectric layer, marked as a shadow in Fig. 1b). These holes are in partial contact with the electrodes, pinning down the position of the droplets. Because of the lateral electric field, the operating voltage is independent of the cell gap. The liquid-2 is used to balance the gravity effect of liquid-1 and also lubricate the surface of the bottom surface.

According to Kelvin's theory, when a liquid droplet experiences an inhomogeneous electric field, if its dielectric constant is different from that of the surrounding medium (gas or liquid), the droplet will bear a dielectric force which can be expressed as[24]

$$F = -\frac{1}{2}\varepsilon_0(\varepsilon_2 - \varepsilon_1)\nabla E^2 \quad (1)$$

where ε_0 represents the permittivity of free space, ε_1 and ε_2 represent the dielectric constants of the droplet and the liquid-2, respectively, and E denotes the electric field on the droplet. From eqn (1), the dielectric force exerted on the droplet surface is related to the electric field gradient (∇E^2) and the dielectric constant difference ($\varepsilon_1 - \varepsilon_2$). Due to the cohesive force, particles (molecules) in the droplet will attract tightly to prevent them from separation; also due to the adhesive force the droplet can attach on the bottom substrate surface. To balance the interfacial tension, the cohesive force, and the induced dielectric force, the shape of the droplet has to change. Fig. 1c shows the basic operation mechanism of droplet deformation. When a voltage is applied across the ITO strips (dielectric layer not shown), only the region between the ITO strips but close to the substrate surface generates the highest electric field. If $\varepsilon_1 > \varepsilon_2$, then the droplet border bears the highest dielectric force $\boldsymbol{F}$ along the ITO strip direction. Therefore, the particles (molecules) at the droplet border moving along the ITO strip direction pull the droplet to expand.

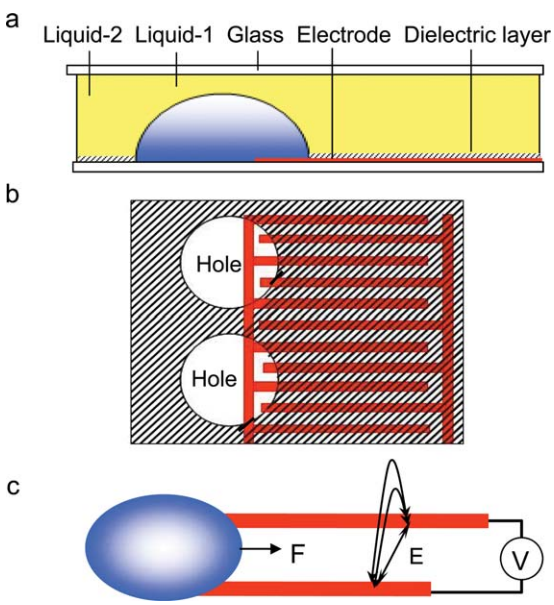

Fig. 1 Structure of the device. a, Side-view. Liquid-1 forms a droplet in the patterned hole on the bottom substrate, and the rest area of the bottom substrate is covered by a dielectric layer. Liquid-2 fills the surrounding of the droplet. These two liquids are sealed by a top glass plate. b, Layout of the interdigitated ITO electrode and the dielectric layer. The holes are used to pin down the droplets. c, spatial electric field (E) distribution across the ITO strips and the generated dielectric force F on the droplet. The hole size and the width of ITO strips are not drawn to scale.

Device fabrication

To prepare a cell as shown in Fig. 1(a), we first etched the ITO electrode on the bottom substrate. The width and gap of the adjacent strips are 10 μm and 10 μm, respectively. We then chose Teflon as the dielectric layer. To fabricate such a hole-patterned Teflon layer as shown in Fig. 1(b), we first dripped small droplets of UV glue (NOA65) on the bottom substrate, partially covering the interdigitated electrode tips. After UV exposure, they were polymerized and firmly fixed to the substrate. Next, we spin-coated the substrate with Teflon solution (400S1-100-1, from DuPont) at 4000 rpm for 20 s, and pre-baked at 120 °C for 5 min. After removing the polymerized NOA65 droplets, we post-baked the substrate at 330 °C for 15 min. The formed Teflon layer presents a very low surface tension ($\gamma \sim 18$ mN m^{-1}) at room temperature.

According to eqn (1), if we choose $\varepsilon_1 > \varepsilon_2$, then the shape of the droplet can be expanded by the fringing field. To choose two liquids, they should be immiscible with each other and their densities match well to minimize the gravity effect. Liquid-1 (droplet) with a relatively low surface tension and a large dielectric constant is preferred for low driving voltage. Liquid-2 should have much lower dielectric constant. Some liquid crystals (LCs) exhibit such properties. Here we chose a commercially available LC mixture, Merck ZLI-4389; its physical properties are listed as follows: $\varepsilon_{//} = 56$, $\Delta\varepsilon = 45.6$, $\gamma \sim 38$ mN m^{-1}, $<n> \sim 1.58$, and $\rho \sim 0.98$ g m^{-3}. We have prepared two LC mixtures; one doped with 1.2 wt% black dye (S-428, from Mitsui Fine Chemicals) and another with 1.2 wt% red dye (Oklahoma dyes C10). When a small volume of the LC mixture forms a droplet in the patterned hole, it exhibits a near-spherical shape with the smallest surface to volume ratio due to the low surface tension of Teflon surface. Then we filled the rest space of the cell with silicon oil ($\varepsilon \sim 2.9$, $\gamma \sim 21$ mN m^{-1}, $n \sim 1.4$, and $\rho \sim 0.97$ g cm^{-3}). Two

glass strips with ~3 mm thickness were placed on the border of the bottom substrate as the spacers. Another glass plate was used to seal the two liquids tightly. The periphery of the cell was sealed by glue.

Dynamic response

When a voltage is applied to the bottom electrodes, a non-uniform lateral electric field (∇E) is generated across the stripes. As a result, a dielectric force is exerted on the LC droplet surface in which there are embedded electrodes. LC molecules on the droplet border are reoriented by the fringing field, so the dielectric constant of the LC on the border is $\varepsilon_{//} = \sim 56$. Such a dielectric constant is much larger than that of the silicon oil. This part of the LC droplet will be stretched outward along the strips. When the LC droplet is big enough, most LC in its bulk exhibit random orientation if the droplet is not stretched to be a thin film. In this case, the LC droplet is polarization insensitive.

Fig. 2 shows such a deformation of a black LC droplet at different voltages. At $V = 0$, the droplet has a near-circular contact area with an aperture of ~1.5 mm on the bottom substrate. The touching area on the bottom substrate surface is the droplet aperture. In this case, the droplet presents the smallest surface–volume ratio. When the voltage is gradually increased to 35 V_{rms}, the droplet begins to stretch along the strip electrodes. At $V = 45$ V_{rms}, the deformation becomes more noticeable. Further expanding goes on with the increased voltage. Compared to the original surface area at $V = 0$, the black dispersed area is expanded by ~1.5× at $V = 50$ V_{rms}, and ~2.5× at $V = 60$ V_{rms}, respectively. Removing the voltage, the droplet quickly returns to its original position and the initial shape because of the pulling of the interfacial tension force of the droplet.

The switching time was measured by monitoring the time-dependent transmitted light intensity in a dark room. A collimated He–Ne laser beam ($\lambda = 633$ nm) is normally incident upon the ITO electrode area closely adjacent from the droplet, as shown in Fig. 3a. At $V = 0$, the beam goes through the cell with the highest transmittance. When a high enough voltage

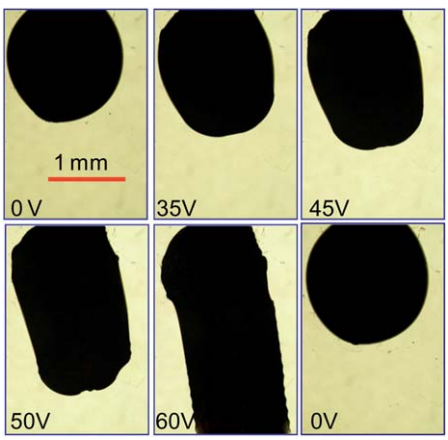

Fig. 2 Surface deformation of a LC droplet (aperture: 1.5 mm) at different voltages. The LC droplet is doped with 1.2 wt% black dye and its outside space is filled with silicon oil. The photographs were taken through an optical microscope. The scale bar is 1 mm.

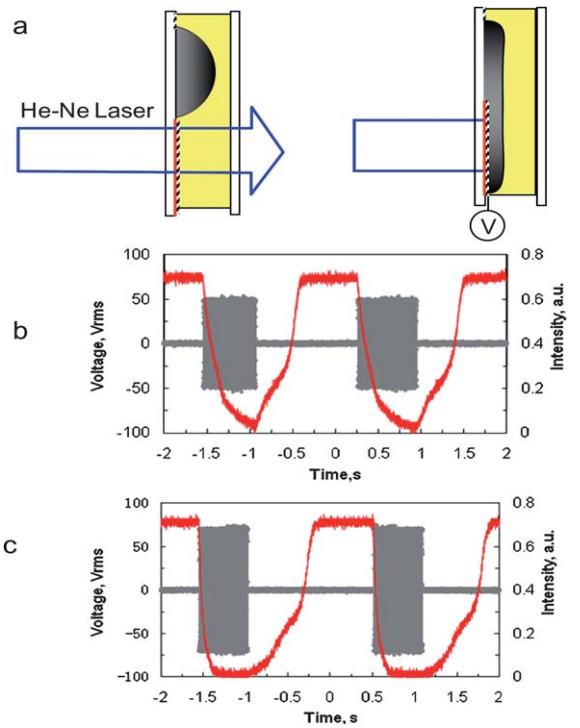

Fig. 3 Schematic experimental setup for measuring the response time and the corresponding experimental results. a, Contracting and expanding droplet for dynamic switching a He–Ne laser beam. b, Recorded transmitted light intensity at 50 V_{rms} voltage bursts. c, Same as b but at 70 V_{rms}. The red lines denote the transmitted light intensity and grey lines the applied voltage.

(>35 V_{rms}) is applied, the droplet is stretched outward, partially blocking the probing beam. The droplet shape depends on the dielectric stretching force. As the dielectric stretching force increases, the radius of curvature of the stretched liquid droplet will gradually increase. The resulting transmitted light intensity is detected by a photodiode and recorded by an oscilloscope.

As Fig. 3b and Fig. 3c show, the expanding and relaxing time are respectively measured as ~0.62 s and ~0.53 s at a 50 V_{rms} (500 Hz) burst, and ~0.17 s and 0.83 s at a 70 V_{rms} (500 Hz) burst. The expanding (relaxing) time is defined as the time needed from the contracting (expanding) shape to a stable stretched (contracting) shape. A higher voltage leads to a longer droplet stretching, however, adversely making the recovery time longer. The cycle driving with two periods shows that the LC droplet returns to its original state quite well. At $V = 50$ V_{rms}, the stretched droplet does not fully block the laser beam, leading to some light leakage (shown in Fig. 3b). As a comparison, at $V = 70$ V_{rms}, the relatively low light transmittance (shown in Fig. 3c) indicates that the expanded area of the droplet is already large enough to totally block the laser beam. The highest intensity was measured to be ~0.72 and the lowest intensity in dark room was ~0.06, leading to a contrast ratio of ~120 : 1 in transmissive mode.

To study the switching time of droplets with different sizes, larger LC droplets were first prepared. The left and right LC droplets in Fig. 4a were doped with black and red dyes, respectively. The aperture of each droplet is ~1.9 mm and they are separated by a ~0.9 mm gap. At $V = 0$, the two droplets contract

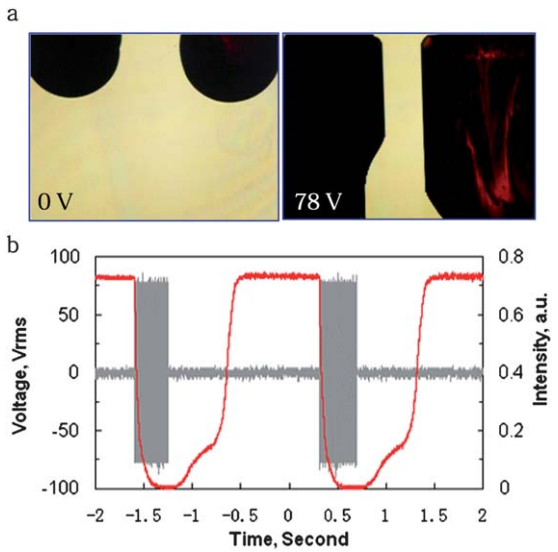

Fig. 4 a, Surface deformation of two LC droplets (aperture: 1.9 mm) at $V = 0$ and $V = 78$ V_{rms}, the left droplet shows black and the right shows red. b, Recorded transmittance at 78 V_{rms} voltage bursts. A video of dynamically deforming the droplet is also provided in the ESI.† The operating voltage was gradually increased or decreased.

in the holes, and have a tendency to stretch along the electrode when the voltage is increased, which is similar to that shown in Fig. 2. At $V = 78$ V_{rms}, the two droplets were extensively stretched along the electrode. One notices that there is still a large gap between the two stretched droplets. At a 78 V_{rms} burst, the measured spreading and recovering time are 0.39 s and 0.70 s, respectively, as Fig. 4b shows. This larger droplet is still greatly expanded by a voltage even with shorter pulse duration. The incident laser beam is switched on and off smoothly with a high contrast ratio. The expanded area at a 78 V_{rms} burst is estimated to be ~3.5×, and the corresponding switchable aperture ratio is ~71%. When the voltage is removed, the transmitted intensity firstly keeps constant for a while (~0.14 s), then starts to increase as Fig. 4b shows. This implies that the expanded droplet occupies a much larger area than the laser beam does. Only when the stretched border of the droplet meets the laser beam, the intensity begins to show an increase. After the 0.14 s delay, it follows by a relatively slow relaxation (0.4 s) which brings transmittance back to ~20% of the original level. This is perhaps due to the relatively large resistance originating from the friction at the liquid–liquid interface. After this relaxation, it takes the droplet ~0.16 s to completely depart the laser beam. This is because the expanding area of the droplet shrinks quickly and the surface tension rather than the friction force plays the main role.

For the right droplet, it still presents dark red under the 78 V_{rms} actuation, which indicates that the expanded LC layer is still very thick.

To estimate the travel speed of the 1.9-mm-aperture droplet, its expanded area at 70 V_{rms} is ~3×, and the measured spreading and recovering times are 0.39 s and 0.70 s respectively. Thus the corresponding speeds are estimated to be ~4.5 mm s^{-1} and ~2.6 mm s^{-1}. respectively. Such results are comparable to the electrofluidic display based on electrowetting mechanism (~2.65 mm s^{-1}).

From Fig. 4a, increasing the voltage can further stretch the LC droplet and enlarge the switchable aperture ratio. However, this also reduces the residual droplet volume in the patterned hole. If we suddenly remove the high operating voltage on an extremely deformed droplet, the friction between the droplet and the surrounding silicon oil begins to play an important role in the relaxation process. As a result, the droplet may be lifted off from the hole and no longer returns to its original position.

To spread a droplet sidewise, zigzag interdigitated electrodes were adopted. The width and gap of the zigzag electrodes are 10 μm and 12 μm, respectively, and the bending angle is 30°. The electrode length between the two bending points is 100 μm. The cell fabrication process is similar to that of the above two cells. Two droplets (left black and right red) were sequentially adhered at one edge of the electrode. The aperture of each droplet is about ~1.2 mm with a separation of 0.9 mm between them. At $V = 0$, the two droplets exhibit a contracted near-spherical shape, as shown in Fig. 5a. As the voltage increases to $V = 50$ V_{rms}, they expand in both elongated and sidewise directions, as shown in Fig. 5b. Although the size of the two droplets are smaller than the droplet shown in Fig. 4, one can see the gap between the stretched droplets becomes much narrower than that shown in Fig. 4a. Using zigzag electrodes, the switchable aperture ratio of the droplet will be enhanced.

Dye-doped droplets with voltage-stretchable surfaces have a potential application for intensity modulations, such as optical switches and displays. Such a droplet can be considered as an elastomeric rubber string, with one end fixed by the substrate surface and the other stretched by the generated dielectric force. Considering one droplet as a pixel, the gray scale is induced by stretching a black or coloured LC droplet from a small circular visible area to different extent. The contrast ratio depends on the thickness of the area covered by LC and the doped dye concentration. A high dye concentration will lead to a large absorption even though the stretched LC layer is thin. Moreover, the same device concept can be extended to other liquids which satisfy the abovementioned criteria. This gives potential for novel liquid displays with polarization insensitive, large viewing angle, high contrast ratio, and multi-stability. Both transmissive and reflective mode can be configured. In display applications, the droplet size is usually smaller than 1 mm, thus the driving voltage and the response time will not be a concern. For a smaller droplet, the response speed will exhibit much faster. The response

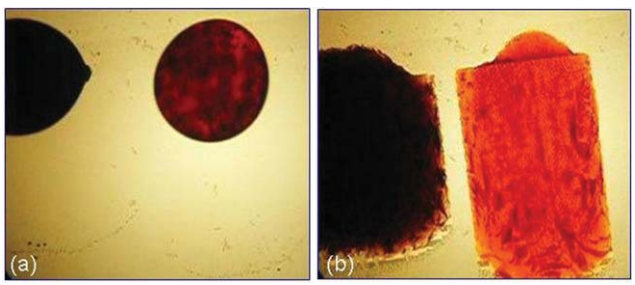

Fig. 5 Two droplets deformed by zigzag striped electrode showing expansion in both elongated and sidewise directions. Left droplet is black and the right one is red. a, at $V = 0$ and b, $V = 50$ V_{rms}. A video of dynamically deforming two droplets is provided in the ESI.† The operating voltage was gradually increased or decreased.

speed has a relationship with the liquid interfacial tension force, the flowing viscosity, as well as the travel distance. A droplet which travels a longer distance usually needs a longer expanding time. To further decrease the operating voltage, interdigitated ITO electrodes with a smaller striped gap can be considered.

From the above experimental results, the selected ZLI-4389 material plays a key role in our device. Such a LC material exhibits a high dielectric constant and medium surface tension. Therefore, its droplet can be extremely stretched by external voltage even though the droplet size is large. If the LC droplet is replaced by an isotropic liquid, then the results will be quite different. For most liquids with low surface tensions, their dielectric constants ($\varepsilon_L \sim 5$) match that of the surrounded liquid (silicon oil $\varepsilon \sim 2.9$), so the droplet is difficult to be deformed by a high voltage. For the liquids with a high dielectric constant (such as water $\varepsilon_W \sim 80$ and glycerol $\varepsilon_G \sim 47$), their surface tensions are usually very high (both over 60 mN m^{-1}) at room temperature. The shape of the droplet is also difficult to be largely changed even though the applied voltage is very high.[17,7,25]

The stability of the LC droplet on the Teflon hole is also important for practical applications. Due to the adhesion of the bottom substrate surface and the support of the surrounding silicon oil, the LC droplet can be firmly fixed in the Teflon hole area. Also the gravity effect on distorting the droplet shape is not a concern even though the size of the droplet is large. In our experiments, the pinning stability of the droplets was preliminarily examined; the droplets were firmly pinned upon the patterned holes on the Teflon surface, even when the surrounding silicon oil was removed. Because a single droplet is too small for practical applications, the future development points towards a large-scale droplet array. These droplets should be separated by a patterned grid (such as black matrices) to avoid the crosstalk. The next technical challenge is to ensure the manufacturability of a uniform hole array on the thin Teflon layer and uniform droplets in the holes. Because we choose a nonconductive liquid crystal as the droplets, the power consumption is fairly low, similar to a conventional liquid crystal device or the level using zone-patterned ITO electrode for driving a LC lens reported in ref. 6.

Conclusion

This work has reported the use of DEP force to deform the shape of large liquid droplets. Based on this new approach and choosing LC with high dielectric constant, the surface of the LC droplet could be extremely expanded from a contracting shape to a film-like shape. To generate a DEP force, interdigitated strip electrodes on one substrate surface are adopted, so that the electrode could provide a large gradient of electric field. Using interdigited strip electrodes, the operating voltage is independent of the cell gap and the size of the droplet is scalable. In voltage-on state, the generated dielectric force stretches the near-spherical LC droplet to a film-like layer without the concern of contacting angle saturation. By removing the voltage, the pinning effect of the bottom substrate and the interfacial surface tension of the two liquids restore the stretched droplet to its original shape. Such a shape stretching is reproducible and stable when the voltage remains on. Zigzag interdigitated strip electrodes further widen the spreading area of the droplet. Doping black or coloured dyes into the droplet, the expanded LC layer can perform as a white or coloured light switch. Polarization independence, broadband, and high contrast ratio are the key features of such a device. This kind of device may find numerous applications in high performance optical switches, displays, and other lab-on-a chip devices.

To dynamically observe the device operation, two videos showing the droplets' expansion and relaxation processes are available as Supplementary Information.†

Acknowledgements

H. Ren is supported by the National Research Foundation of Korea (Basic Science Research Program 2010-0021680), and the University of Central Florida group is indebted to the US Air Force Office of Scientific Research (AFOSR) for partial financial support under contract No. FA95550-09-1-0170.

References and notes

1 M. Schadt and W. Helfrich, *Appl. Phys. Lett.*, 1971, **18**, 127–128.
2 B. Berge and J. Peseux, *Eur. Phys. J. E.*, 2000, **3**, 159–163.
3 T. Krupenkin, S. Yang and P. Mach, *Appl. Phys. Lett.*, 2003, **82**, 316–318.
4 S. Kuiper and H. W. Hendriks, *Appl. Phys. Lett.*, 2004, **85**, 1128–1130.
5 S. Grilli, L. Miccio, V. Vespini, A. Finizio, S. De Nicola and P. Ferraro, *Opt. Express*, 2008, **16**, 8084–8093.
6 C. C. Cheng, C. A. Chang and J. A. Yeh, *Opt. Express*, 2006, **14**, 4101–4106.
7 H. Ren, H. Xianyu, S. Xu and S. T. Wu, *Opt. Express*, 2008, **16**, 14954–14960.
8 S. A. Reza and N. A. Riza, *Opt. Commun.*, 2009, **282**, 1298–1303.
9 H. Ren, S. Xu, D. Ren and S. T. Wu, *Opt. Express*, 2011, **19**, 1985–1990.
10 N. R. Smith, D. C. Abeysinghe, J. W. Haus and J. Heikenfeld, *Opt. Express*, 2006, **14**, 6557–6563.
11 Y. J. Lin, K. M. Chen and S. T. Wu, *Opt. Express*, 2009, **17**, 8651–8656.
12 C. G. Tsai and J. A. Yeh, *Opt. Lett.*, 2010, **35**, 2484–2486.
13 R. A. Hayes and B. J. Feenstra, *Nature*, 2003, **425**, 383–385.
14 J. Heikenfeld, K. Zhou, E. Kreit, B. Raj, S. Yang, B. Sun, A. Milarcik, L. Clapp and R. Schwartz, *Nat. Photonics*, 2009, **3**, 292–296.
15 L. Dong, A. K. Agarwal, D. J. Beebe and H. Jiang, *Nature*, 2006, **442**, 551–554.
16 C. A. López, C. C. Lee and A. H. Hirsa, *Appl. Phys. Lett.*, 2005, **87**, 134102.
17 F. Mugele and J. C. Baret, *J. Phys.: Condens. Matter*, 2005, **17**, 705–774.
18 C. V. Brown, G. G. Wells, M. I. Newton and G. McHale, *Nat. Photonics*, 2009, **3**, 403–405.
19 N. Demierre, T. Braschler, P. Linderholm, U. Seger, H. van Lintel and P. Renaud, *Lab Chip*, 2007, **7**, 355–365.
20 K. Park, H.-J. Suk, D. Akin and R. Bashir, *Lab Chip*, 2009, **9**, 2224–2229.
21 K.-L. Wang, T. B. Jones and A. Raisanen, *Lab Chip*, 2009, **9**, 2319–2325.
22 T. B. Jones, M. Gunji, M. Washizu and M. J. Feldman, *J. Appl. Phys.*, 2001, **89**, 1441–1448.
23 L. Wang, L. A. Flanagan, N. Li Jeon, E. Monuki and A. P. Lee, *Lab Chip*, 2007, **7**, 1114–1120.
24 P. Penfield and H. A. Haus, *Electrodynamics of Moving Media*, MIT, Cambridge, 1967.
25 S. Xu, Y. J. Lin and S. T. Wu, *Opt. Express*, 2009, **17**, 10499–10505.

